



HAL
open science

Magnetization-induced second harmonic generation enhanced by surface plasmons in Au/Co/Au ultrathin films

Gilles Tessier, C. Malouin, Patrick Georges, Alain Brun, D. Renard, V. V. Pavlov, P. Meyer, J. Ferre, Pierre Beauvillain

► **To cite this version:**

Gilles Tessier, C. Malouin, Patrick Georges, Alain Brun, D. Renard, et al.. Magnetization-induced second harmonic generation enhanced by surface plasmons in Au/Co/Au ultrathin films. *Applied Physics B - Laser and Optics*, 1999, 68 (3), pp.545-548. 10.1007/s003400050663 . hal-00761550

HAL Id: hal-00761550

<https://hal-iogs.archives-ouvertes.fr/hal-00761550>

Submitted on 26 Aug 2022

HAL is a multi-disciplinary open access archive for the deposit and dissemination of scientific research documents, whether they are published or not. The documents may come from teaching and research institutions in France or abroad, or from public or private research centers.

L'archive ouverte pluridisciplinaire **HAL**, est destinée au dépôt et à la diffusion de documents scientifiques de niveau recherche, publiés ou non, émanant des établissements d'enseignement et de recherche français ou étrangers, des laboratoires publics ou privés.



Distributed under a Creative Commons Attribution - NonCommercial 4.0 International License

Magnetization-induced second-harmonic generation enhanced by surface plasmons in ultrathin Au/Co/Au metallic films

G. Tessier^{1,*}, C. Malouin¹, P. Georges¹, A. Brun¹, D. Renard¹, V.V. Pavlov², P. Meyer³, J. Ferré³, P. Beauvillain⁴

¹Institut d'Optique Théorique et Appliquée, URA CNRS 14, Bât. 503, Université de Paris-Sud, 91403 Orsay Cédex, France

²A.F. Ioffe Physical Technical Institute of the Russian Academy of Sciences, 194021 St. Petersburg, Russia

³Laboratoire de Physique des Solides, URA CNRS 02, Bât. 510, Université de Paris-Sud, 91405 Orsay Cédex, France

⁴Institut d'Électronique Fondamentale, URA CNRS 22, Bât. 220, Université de Paris-Sud, 91405 Orsay Cédex, France

Abstract. Magnetization-induced second-harmonic generation near the surface plasmon resonance in an ultrathin Au/Co/Au structure has been investigated. The resonant coupling of surface plasmons at the fundamental frequency results in a strong enhancement and sign reversal of the nonlinear magneto-optical effects. Model calculations of the observed phenomena are given on the basis of a nonlocal field theory which permits the different interface contributions to the nonlinear polarization $\mathbf{P}^{(2\omega)}$ to be distinguished.

PACS: 78.20.Ls; 42.65.Ky; 71.45.Gm; 78.66.-w

Surface plasmons (SP) are surface electromagnetic waves which can be excited in noble metals below the plasma frequency [1]. It has been shown experimentally and theoretically that optical second-harmonic generation (SHG) is strongly enhanced near the SP resonance [1–5]. In the last few years great attention has been paid to the study of thin magnetic multilayer structures due to their novel physical properties, like giant magnetoresistance and interlayer anti-ferromagnetic coupling, and their large potential for technical applications. The resonant coupling of the electric field at optical frequencies with SP in metallic multilayer films results in an increase of the linear magneto-optical effects [6]. Since the first observation of magnetization-induced SHG [7, 8] (also called NOMOKE for the nonlinear magneto-optical Kerr effect) it has been proven that SHG is a powerful method for studying magnetic surfaces and interfaces. This method was intensively used for investigations of new nonlinear magneto-optical phenomena in different film compositions [9–14], showing that magnetization-induced SHG is very sensitive to the magnetic and electronic structure of thin films.

In this article we present the first experimental observation of nonlinear magneto-optical phenomena near the surface plasmon resonance in ultrathin Au/Co/Au multilayer films. The measurements were done using the attenuated

total reflection (ATR) technique in the Kretschmann geometry [15]. The resonant coupling of SP with light at the fundamental frequency gives rise to a strong enhancement of the total SHG, as compared to the classical reflection configuration used in [7–13]. The magnetization-induced SHG is also enhanced, and exhibits a sign reversal near the SP resonance. We developed a model on the basis of a nonlocal field theory, which allows us to distinguish the contributions of the various interfaces to SHG. Model calculations are in very good agreement with the observed phenomena.

In the electric-dipole approximation, SHG is only allowed in media lacking space-inversion symmetry [16]. For noncentrosymmetric media possessing magnetization \mathbf{M} , the nonlinear polarization $\mathbf{P}^{(2\omega)}$ can be expressed as

$$P_i^{(2\omega)} = \varepsilon_0 \chi_{ijk}^{(i)} E_j E_k \pm \varepsilon_0 \chi_{ijk}^{(c)} (\pm \mathbf{M}) E_j E_k, \quad (1)$$

where E_j and E_k are components of the optical electric field at the fundamental frequency ω . The first term in (1) describes the time-invariant (*i*-type [17]) nonmagnetic contribution to $\mathbf{P}^{(2\omega)}$. The second term in (1) contains the time-noninvariant (*c*-type [17]) nonlinear susceptibility $\chi_{ijk}^{(c)}$ which gives rise to new nonlinear phenomena such as nonlinear magneto-optical rotation [9] and nonlinear circular dichroism [18]. This term changes sign under the time-reversal operation, and is therefore an odd function of the magnetization \mathbf{M} . Neglecting dissipation in the medium, $\chi_{ijk}^{(i)}$ is a real tensor and $\chi_{ijk}^{(c)}$ is a pure imaginary tensor [19]. In the presence of absorption $\chi_{ijk}^{(i)}$ and $\chi_{ijk}^{(c)}$ are complex, thus allowing interference between them. For crystallographically centrosymmetric layers SHG is allowed, in the electric-dipole approximation, only at surfaces and interfaces where the space-inversion symmetry is broken. The nonlinear optical polarization $\mathbf{P}^{(2\omega)}$ excited in a three-photon process ($\hbar\omega_2 = \hbar\omega_1 + \hbar\omega_1$) is the source term for the SH intensity [16]:

$$I^{(2\omega)} \propto |\chi^{(i)}|^2 + |\chi^{(c)}|^2 \pm 2 |\chi^{(i)}| |\chi^{(c)}| \cos \varphi, \quad (2)$$

where φ is the optical phase difference between *i*- and *c*-type nonlinear susceptibilities. When the magnetization \mathbf{M} is re-

* E-mail: Gilles.Tessier@iota.u-psud.fr

versed, φ changes by 180° and the sign of the interference term $2|\chi^{(i)}||\chi^{(c)}|\cos\varphi$ is changed [13].

The ultrathin Au/Co/Au films were deposited on a 1-mm-thick float glass substrate in a high vacuum chamber, following the procedure described in [20]. The first 25 nm-thick Au buffer layer was used to obtain large *fcc* crystallites and to reduce the surface roughness. The second 3 nm-thick (15 monolayers) Co layer had a polycrystalline *hcp* structure with (0001) planes parallel to the film surface. This Co layer was protected by a 3-nm-thick Au top layer. At such Co thickness, the easy magnetization axis was parallel to the surface of the film. Pulsed coils producing an in-plane magnetic field up to 1 kOe were specially designed to magnetize this sample. The glass substrate was optically coupled to a half-cylindrical glass lens by using a refractive index adaptation liquid.

The experimental setup and the geometry of measurements in ATR configuration are shown in Fig. 1. The mode-locked Ti:sapphire laser pumped by an Ar-laser was used as a source of 100 fs light pulses with a repetition frequency of 86 MHz at the wavelength of $\lambda = 800$ nm. The beam, with an average power of 30 mW, was focused on the sample in a spot of about 100 μm in diameter. In front of the sample, a RG715 filter was used in order to eliminate possible parasitic SHG generated at the surfaces of the optical elements. After the sample we used a BG40 filter to block the fundamental light. The SH intensity generated by the Au/Co/Au film was measured with a high-sensitivity cooled CCD camera. We used *p*-polarized fundamental light (TM mode) which excites SP near an incidence angle θ_p with a wave vector k_p defined by the SP dispersion equation [1]

$$k_p = \frac{\omega}{c} \sqrt{\frac{\varepsilon_1 \varepsilon_2}{\varepsilon_1 + \varepsilon_2}}, \quad (3)$$

where ε_1 and ε_2 are the dielectric constants of the two media at the interface at which SP are excited. SP may be coupled with evanescent optical waves from a half-cylindrical glass lens at the angle

$$\theta_p = \arcsin\left(\frac{k_p c}{\omega \sqrt{\varepsilon}}\right), \quad (4)$$

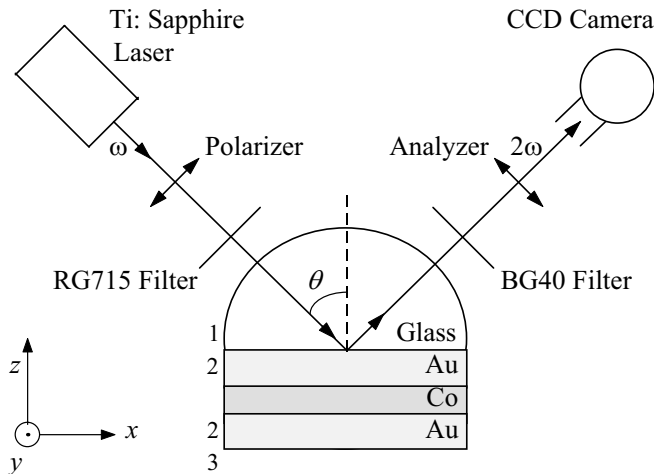


Fig. 1. Schematics of the experimental setup

where ε is the dielectric constant of the glass. For interfaces between optically isotropic media with *p*-polarized excitation, when there are only *x* and *z* components in the fundamental electric field (see Fig. 1), the nonlinear polarization $\mathbf{P}^{(2\omega)}$ can be described for the longitudinal geometry ($\mathbf{M}\parallel x$) by the matrix expression

$$\begin{pmatrix} P_x^{(2\omega)} \\ P_y^{(2\omega)} \\ P_z^{(2\omega)} \end{pmatrix} = \varepsilon_0 \begin{pmatrix} 0 & \chi_{xxz}^{(i)} & 0 \\ \chi_{yxx}^{(c)} & 0 & \chi_{yzz}^{(c)} \\ \chi_{zxx}^{(i)} & 0 & \chi_{zzz}^{(i)} \end{pmatrix} \begin{pmatrix} E_x^2 \\ 2E_x E_z \\ E_z^2 \end{pmatrix}. \quad (5)$$

For the transversal geometry, when $\mathbf{M}\parallel y$, $\mathbf{P}^{(2\omega)}$ can be written as

$$\begin{pmatrix} P_x^{(2\omega)} \\ P_y^{(2\omega)} \\ P_z^{(2\omega)} \end{pmatrix} = \varepsilon_0 \begin{pmatrix} \chi_{xxx}^{(c)} & \chi_{xxz}^{(i)} & \chi_{xzz}^{(c)} \\ 0 & 0 & 0 \\ \chi_{zxx}^{(i)} & \chi_{zxz}^{(c)} & \chi_{zzz}^{(i)} \end{pmatrix} \begin{pmatrix} E_x^2 \\ 2E_x E_z \\ E_z^2 \end{pmatrix}. \quad (6)$$

The nonzero *i*- and *c*-type tensor elements of the nonlinear susceptibility χ_{ijk} are obtained on the basis of symmetry considerations [17]. It is important to note that for *p*-excitation in the longitudinal geometry, the SH field corresponding to $\mathbf{P}^{(2\omega)}$ is *p*-polarized for the nonmagnetic (*i*-type) contribution, and *s*-polarized for the magnetic (*c*-type) one, whereas in the transversal geometry SHG is always *p*-polarized. These symmetry properties of the nonlinear susceptibilities are responsible for the nonlinear magneto-optical rotation observed in [9].

The variations of the reflectivity of the Au/Co/Au film at the fundamental light frequency versus the angle of incidence are shown in Fig. 2a. The signal increases up to the total internal reflection angle $\theta_t \simeq 43.5^\circ$ and then strongly decreases down to the angle $\theta_p \simeq 45^\circ$. The sharp minimum in the intensity of the reflected light indicates that SP are excited near this angle. Similar behavior of the reflected light at $\lambda = 632.8$ nm in Au/Co/Au film has already been observed by Safarov et al. [6]. Theoretical modeling of the reflection coefficients and magneto-optical effects in Au/Co/Au films in the ATR configuration on the basis of a nonlocal field approach has been achieved by Kosobukin [21]. It was established that in the Au/Co/Au/glass structure SP are excited at the air-Au interface. The coupling of the light with SP gives rise to a strong enhancement of the magneto-optical response measured by the linear Kerr effect and by near field microscopy [6].

The total SH intensity measured in longitudinal geometry ($\mathbf{M}\parallel x$) with *p*-polarized input and *p*-polarized output is shown by dots in Fig. 2b for angles ranging from 40.5° to 48.5° . According to (5) there is no magnetic contribution to the nonlinear polarization in this configuration. The SH signal has a strong minimum at the angle $\theta \simeq 44^\circ$. It reaches a maximum near θ_p , decreases, and is constant for angles $\theta > 47^\circ$.

The dots in Fig. 3 represent the SH magnetic contrast ϱ , measured in longitudinal geometry ($\mathbf{M}\parallel x$) for $\theta = 45.2^\circ$, as a function of the angular position α of the analyzer ($\alpha = 0$ corresponds to *p*-polarization), where ϱ is defined as

$$\varrho = \frac{I^{(2\omega)}(+\mathbf{M}) - I^{(2\omega)}(-\mathbf{M})}{I^{(2\omega)}(+\mathbf{M}) + I^{(2\omega)}(-\mathbf{M})} = \frac{2|\chi^{(i)}||\chi^{(c)}|\cos\varphi}{|\chi^{(i)}|^2 + |\chi^{(c)}|^2}. \quad (7)$$

The SH magnetic contrast ϱ is proportional to the nonlinear susceptibilities $\chi^{(i)}$ and $\chi^{(c)}$ and does not depend on the intensity of the fundamental frequency light. The experimental

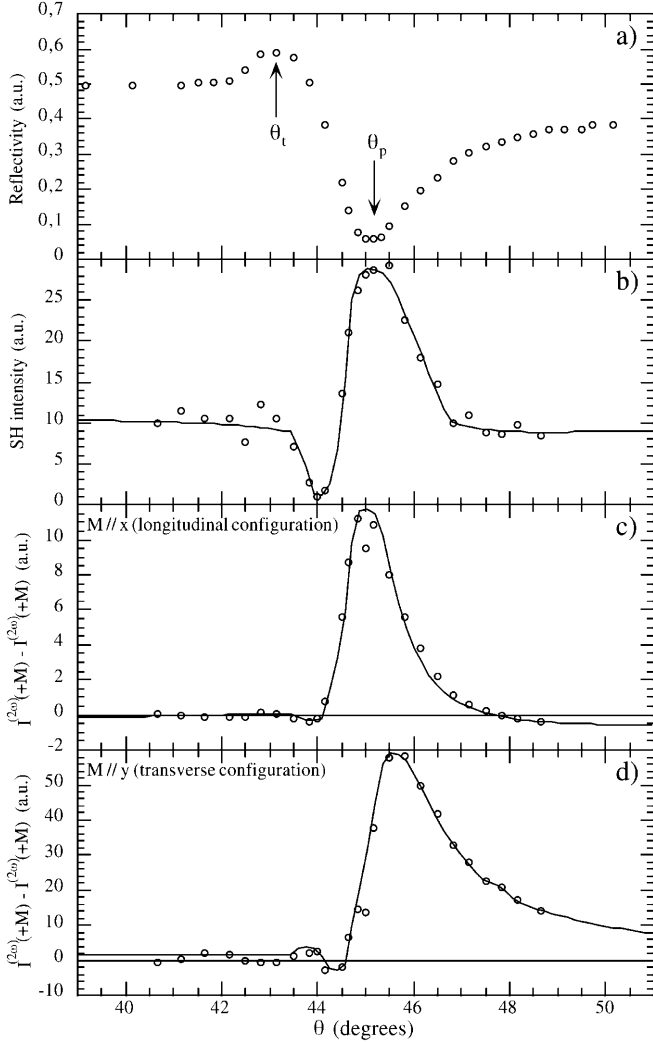


Fig. 2a-d. Variations with the incidence angle θ of the reflectivity at the fundamental frequency (a), the nonmagnetic SHG intensity (b), the magnetization-induced part of the SHG, $I^{(2\omega)}(+M) - I^{(2\omega)}(-M)$, in longitudinal (c) and transversal (d) geometries

data are fitted by an equation given in [10]:

$$\varrho = \frac{2\Phi \tan \alpha \cos \varphi}{1 + (\Phi \tan \alpha)^2}, \quad (8)$$

where Φ is the ratio and φ the phase difference between the magnetic and nonmagnetic nonlinear susceptibilities given in (5). The best fit, shown by the solid line in Fig. 3, gives the following parameters: $\Phi = 0.045 \pm 0.001$, $\varphi = 68.2^\circ \pm 0.3^\circ$. Thus the longitudinal configuration as well as the polar geometry [10] allow the measurement of the important nonlinear magneto-optical parameters Φ and φ , which are related to the nonlinear rotation and ellipticity [9, 10]. One should mention that in the transparency region of a medium $\varphi = 90^\circ$. In this case the interference between i - and c -type contributions is not allowed and it becomes difficult to distinguish the magnetic contribution to the SH intensity.

We define the magnetization-induced part of the SH light as the difference between the SH intensities for two opposite magnetizations: $I^{(2\omega)}(+M) - I^{(2\omega)}(-M) \propto |\chi^{(i)}| |\chi^{(c)}| \cos \varphi$. The

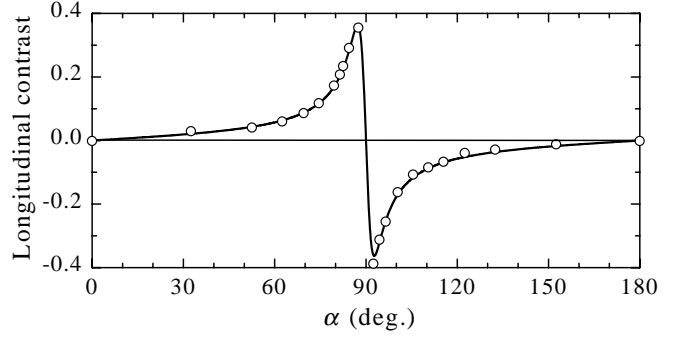


Fig. 3. Longitudinal magnetic contrast of SHG as a function of the azimuthal position α of the analyzer. $\alpha = 0$ corresponds to p -polarization

dots in Fig. 2c show this magnetization-induced part of the SH light in the longitudinal configuration versus the angle θ , for the position of the analyzer $\alpha = 80^\circ$ where we obtained a good signal-to-noise ratio. The magnetization-induced SH signal changes sign twice in the narrow angle interval $\theta_t < \theta < 44.5^\circ$, and then has a broad maximum near the angle of SP excitation θ_p . It decreases drastically for larger angles of incidence and then changes sign at $\theta \simeq 48^\circ$. The same type of measurements were performed in transverse configuration ($M \parallel y$) for p -input and s -output polarizations and are shown in Fig. 2d. The sign of the transverse magnetization-induced SH signal changes twice in the angle interval $\theta_t < \theta < 45^\circ$. Then it increases strongly and has a broad maximum at $\theta \simeq 45.5^\circ$.

In order to explain our results, we developed a model involving multiple interferences of the different contributions to the fundamental and SH electric fields. The fact that the E_z component of the electric field and the characteristics of the media are treated as discontinuous in the macroscopic limit, although they vary physically on an atomic scale throughout a transition layer, led us to consider a nonlocal theory. This theory was developed for trilayer metallic systems near the SP resonance in [21, 22]. An incident monochromatic light at the fundamental frequency ω has an electric field $\mathbf{E}(\omega, \mathbf{r})$, which is related to a polarization $\mathbf{P}(\omega, \mathbf{r})$ excited in the medium according to the wave equation

$$\text{rot rot} \mathbf{E}(\omega, \mathbf{r}) - k_0^2 \varepsilon^0(z, \omega) \mathbf{E}(\omega, \mathbf{r}) = 4\pi k_0^2 \mathbf{P}(\omega, \mathbf{r}), \quad (9)$$

where $k_0 = \omega/c$, the dielectric function $\varepsilon^0(z, \omega)$ is equal to $\varepsilon_1(\omega)$ if $z < 0$ (the glass substrate and the glass prism), $\varepsilon_2(\omega)$ if $0 < z < L$ (the gold film) and ε_3 if $z > L$ (air). In the case of a nonlinear medium the electric polarization $\mathbf{P}(\omega, \mathbf{r})$ is written as

$$\mathbf{P}(\omega, \mathbf{r}) = \mathbf{P}(\omega, \mathbf{r}) + \mathbf{P}(2\omega, \mathbf{r}) + \dots \quad (10)$$

Following [22], (9) can be solved for the Fourier component $\mathbf{E}(\omega, \mathbf{r}) = \mathbf{E}(z; \omega, \mathbf{k}) \exp(i\mathbf{k}x)$ corresponding to the wave vector $\mathbf{k} = \mathbf{e}_x k_0 \sqrt{\varepsilon_1(\omega)} \sin \theta$, where \mathbf{e}_x is the unit vector along the x axis. Generally for a weak nonlinearity the Fourier component of the polarization $\mathbf{P}^{2\omega}(z; 2\omega, 2\mathbf{k})$ can be written as

$$P_i(z; 2\omega, 2\mathbf{k}) = (2\pi)^3 \iint \chi_{ijk}^{(2)}(z, z_1, z_2; \omega, 2\omega, \mathbf{k}, 2\mathbf{k}) E_j(z_1; \omega, \mathbf{k}) E_k(z_2; \omega, \mathbf{k}) dz_1 dz_2 \quad (11)$$

The nonlinear susceptibility $\chi_{ijk}^{(2)}$ is assumed to be nonlocal in z . The functions E_j and E_k are discontinuous at the film interfaces due to the boundary conditions. Following the nonlocal approach we use the continuous functions F_j and F_k for the fundamental electric field of the light which results from self-consistent solutions of the wave equations [21]. We can write the electric field of the light at double frequency as

$$E_i^{(2\omega)}(z; 2\omega, 2\mathbf{k}) = A_{ijk}(z; \omega, 2\omega, \mathbf{k}, 2\mathbf{k}) F_j(z; \omega, \mathbf{k}) F_k(z; \omega, \mathbf{k}) \quad (12)$$

where the tensor A_{ijk} includes integral function of the nonlinear susceptibility $\chi_{ijk}^{(2)}$. The continuous functions F_j and F_k are calculated on the basis of the Green functions and given in [21] for the interfaces of trilayer films. In order to calculate the total nonlinear electric field generated from a Au/Co/Au film it is necessary to take into account multiple interference of different contributions to SHG. The electric field of the SH wave $E_i(2\omega)$ in the glass prism can be given as a sum of SHG contributions from the film interfaces

$$E_i(2\omega) = A_{ijk}^{21} F_j^{21} F_k^{21} f(\theta) - T^{21} A_{ijk}^{42} F_j^{42} F_k^{42} f(\theta) e^{2iK_2 d_2} \quad (13) \\ + T^{42} T^{21} A_{ijk}^{42} F_j^{24} F_k^{24} f(\theta) e^{2i(K_4 d_4 + K_2 d_2)} \\ + T^{24} T^{42} T^{21} A_{ijk}^{32} F_j^{32} F_k^{32} f(\theta) e^{2i(K_2 d_2' + K_4 d_4 + K_2 d_2)},$$

where T^{ab} are the Fresnel transmission coefficients for SH light. The numbering of the interfaces is given in Fig. 1: 21 is the Au/glass, 24 the Au/Co, 42 the Co/Au and 32 the air/Au interface, d_2 , d_2' and d_4 are the thickness of the Au buffer, Au upper layer and Co layer respectively. The function $f(\theta)$ must be taken as $\cos(\theta)$ or $\sin(\theta)$ for x or z polarizations of the SH light. K_n is the complex z component of the SH wave vector for medium n :

$$K_n = \sqrt{\varepsilon_n(2\omega) K_0^2 - K^2}, \quad (14)$$

where $K_0 = 2\omega/c$, $K = K_0 \sqrt{\varepsilon_1(2\omega)} \sin \theta$. The first term in (13) describes a contribution to $E_i(2\omega)$ from the air-Au interface, the second and third terms are from the Au-Co and Co-Au interfaces, the fourth term is from the air-Au interface. At each film interface in respect with (5) and (6) there are six independent SH components in the transverse geometry and five independent SH components in the longitudinal one for p -polarized fundamental light. We developed a program using (7) and (13) for nonlinear procedures fitting our data. The complex refractive indices of Au and Co were taken from [23], and the unknown components of the tensor A_{ijk} were taken as fit parameters. The calculated curves are shown in Fig. 2b-d by the solid lines. One may see that we obtained very good agreement between experiment and theory. In the experiments presented here, the SH yield obtained by using surface plasmons is enhanced by a factor of four, approximately, as compared to the classical reflection configuration. Nevertheless, there is a considerable temporal broadening of the fundamental pulses due to the spectral dispersion of the thick glass lens which was used to couple surface plasmons into the layers. Using the above model and the calculated parameters, we were able to calculate that an enhancement up to two orders of magnitude could be reached

by pre-compensating the spectral dispersion with an appropriate sequence of prisms.

We have demonstrated experimentally for the first time magnetization-induced second-harmonic generation in the region of the surface plasmon excitation in ultrathin Au/Co/Au structures. In the electric-dipole approximation second-harmonic generation is allowed at magnetic and nonmagnetic interfaces in these films. At the angle θ_p , due to the coupling of SP with the fundamental frequency light, the fundamental electric field is resonantly enhanced at the nonmagnetic air/Au interface and redistributed to the magnetic Au/Co and Co/Au interfaces. This results in a strong enhancement of both the magnetization-induced and the nonmagnetic SHG. Drastic changes in the distribution of the fundamental field at the magnetic interface near θ_p result in a sign reversal of the magnetization-induced part of SHG in longitudinal and transversal geometries. Model calculations based on a nonlocal field theory are shown to be in good agreement with the experimental results.

Acknowledgements. The authors wish to acknowledge funding from the BQR of the Université Paris XI, the TMR-network *ERBFMRXCT98-0015* (NOMOKE), *ULTIMATECH* and *INTAS 94-2675* contracts. The work of V.V.P. was supported by a grant from the *MENRT* and by the *RFBR*. The work of C.M. was supported by the *MAE* (Bourse Brézin). Two of us (V.V.P. and C. M.) would like to thank the *LPS* and the *IOTA* at the Université de Paris-Sud for their hospitality during our stay.

References

1. V.M. Agranovich, D.L. Mills (Eds.): *Surface Polaritons* (North-Holland, Amsterdam 1982)
2. H.J. Simon, D.E. Mitchell, J.G. Watson: *Phys. Rev. Lett.* **33**, 1531 (1974)
3. F. de Martini, Y.R. Shen: *Phys. Rev. Lett.* **36**, 216 (1976); F. de Martini, M. Colocci, S.E. Kohn, Y.R. Shen: *Phys. Rev. Lett.* **38**, 1223 (1977)
4. H.J. Simon, R.E. Benner, J.G. Rako: *Opt. Commun.* **23**, 245 (1977)
5. C.K. Chen, A.R.B. de Castro, Y.R. Shen: *Opt. Lett.* **4**, 393 (1979)
6. V.I. Safarov, V.A. Kosobukin, C. Hermann, G. Lampel, J. Peretti: *Phys. Rev. Lett.* **73**, 3584 (1994)
7. J. Reif, J.C. Zink, C.-M. Schneider, J. Kirschner: *Phys. Rev. Lett.* **67**, 2878 (1991)
8. J. Reif, C. Rau, E. Matthias: *Phys. Rev. Lett.* **71**, 1931 (1993)
9. B. Koopmans, M. Groot Koerkamp, Th. Rasing, H. v. d. Berg: *Phys. Rev. Lett.* **74**, 3692 (1995)
10. M. Straub, R. Vollmer, J. Kirschner: *Phys. Rev. Lett.* **77**, 743 (1996)
11. T.M. Crawford, C.T. Rogers, T.J. Silva, Y.K. Kim: *Appl. Phys. Lett.* **68**, 1573 (1996)
12. A. Kirilyuk, Th. Rasing, R. Mégy, P. Beauvillain: *Phys. Rev. Lett.* **77**, 4608 (1996)
13. R. Stolle, K.J. Veenstra, F. Manders, Th. Rasing, H. v. d. Berg, N. Persat: *Phys. Rev. B* **55**, R4925 (1997)
14. V.V. Pavlov, R.V. Pisarev, A. Kirilyuk, Th. Rasing: *Phys. Rev. Lett.* **78**, 2004 (1997)
15. E. Kretschmann: *Z. Phys.* **241**, 313 (1971)
16. Y.R. Shen: *The Principles of Nonlinear Optics* (Wiley, New York 1984)
17. R.R. Birss: *Symmetry and Magnetism* (North-Holland, Amsterdam 1966)
18. A. Kirilyuk, Th. Rasing, V.N. Gridnev, V.V. Pavlov, R.V. Pisarev (to be published)
19. Ru-Pin Pan, H.D. Wei, Y.R. Shen: *Phys. Rev. B* **39**, 1229 (1989)
20. D. Renard, G. Nihou, *Phil. Mag. B* **55**, 75 (1987)
21. V.A. Kosobukin: *J. Magn. Magn. Mater.* **153**, 397 (1996)
22. V.A. Kosobukin: *Sov. Phys. Tech. Phys.* **31**, 879 (1986)
23. P.B. Johnson, R.W. Christy: *Phys. Rev. B* **6**, 4370 (1972); *Phys. Rev. B* **9**, 5056 (1974)